PNAS
www.pnas.org

Supplementary Information for

Production, composition, and mode of action of the painful defensive venom produced by a limacodid caterpillar, *Doratifera vulnerans*

Andrew A. Walker[1]*, Samuel D. Robinson[1], Jean-Paul V. Paluzzi[2], David J. Merritt[3], Samantha A. Nixon[1,4], Christina I. Schroeder[1†], Jiayi Jin[1], Mohaddeseh Hedayati Goudarzi[1], Andrew C. Kotze[4], Zoltan Dekan[1], Andy Sombke[5], Paul F. Alewood[1], Bryan G. Fry[3], Marc E. Epstein[6], Irina Vetter[1,7], and Glenn F. King[1]*

[1]Institute for Molecular Bioscience, The University of Queensland, St Lucia QLD 4072, Australia
[2]Department of Biology, York University, Toronto, Ontario M3J 1P3, Canada
[3]School of Biological Sciences, The University of Queensland, St Lucia QLD 4072, Australia
[4]CSIRO Agriculture and Food, Queensland Bioscience Precinct, St Lucia QLD 4072, Australia
[5]Department of Evolutionary Biology, Integrative Zoology, University of Vienna, Vienna, Austria 1090
[6]Plant Pest Diagnostics Branch, California Department of Food and Agriculture, Sacramento, CA 95832-1448, USA
[7]School of Pharmacy, The University of Queensland, Woolloongabba QLD 4102, Australia

*Andrew A. Walker
Email: a.walker@imb.uq.edu.au
*Glenn F. King
Email: glenn.king@imb.uq.edu.au

[†]Current address: National Cancer Institute, National Institutes of Health, Frederick, MD 21702

This PDF file includes:

Other supplementary materials for this manuscript include the following:

Movie S1
Dataset S1

Supplementary Methods

Insect collection, culture, and venom harvesting

Caterpillars were collected from *Eucalyptus* sp. trees on private land in Brisbane, Australia. They were maintained in the laboratory at 23°C with a 12 h:12 h light/dark cycle on small *Eucalyptus* branches with the stems immersed in water. Some animals were also bred in the laboratory by allowing moths matured from wild-caught caterpillars to mate and lay eggs on leaves. Venom harvest was performed using cleaned parafilm suspended on a 20 mm × 30 mm wire loop with an extended wire handle. The parafilm was gently pressed onto caterpillars, resulting in the deposition of numerous tiny drops of venom. These drops were recovered by pipetting 20 µL of water onto the parafilm and transferring the liquid to a 1.5 mL tube. After collecting venom from multiple individual caterpillars into a single tube, the liquid was lyophilized, resuspended in ultrapure water, and the concentration estimated using a nanodrop spectrophotometer with conversion factor 1 AU/cm^{-1} = 1 mg/mL. Over the course of this study venom from several hundred caterpillars of the final three instars was harvested and pooled for analysis. Voucher specimens of *D. vulnerans* used in this study were deposited to the Queensland Museum and are awaiting allocation of reference numbers.

Microscopy

Caterpillars were fixed by injection of 3.7% formalin in phosphate-buffered insect saline (PBS) and dissected under fixative solution to isolate the spine-covered scoli. After 30 min fixation, the scoli were washed in PBS, dehydrated through an ethanol series (50–100%) and embedded in LRWhite resin (London Resin Company, Berkshire, UK) in gelatine capsules cured at 60°C for 24 h. Sections of 3 µm thickness were cut using a retracting Rotary One microtome (LKB Bromma, Bromma, Sweden) and glass Ralph knives, floated onto a water:acetone bath, and collected onto a microscope slide where they were dried and stained with toluidine blue at 80°C. Cover-slipped sections were viewed using a Axioskop compound microscope (Zeiss, Oberkochen, Germany) and imaged using a Toupcam ODCM0510C camera and ToupLite software (ToupTek, Hangzhou, Zhejiang, China).

µ-CT imaging

Caterpillars for µ-CT were fixed in Bouin's fixative (71.4% picric acid, 23.8% formalin, 4.8% acetic acid), dehydrated using a graded ethanol series and incubated overnight in 1% alcoholic iodine solution (#X864.1, Carl Roth, Karlsruhe, Germany). After washing in 99.8% ethanol, the specimens were critical point dried using an automated dryer (EM CPD300, Leica Microsystems, Wetzlar, Germany) and mounted on an aluminum SEM stub with a hot glue gun. Scanning was performed using a Zeiss XRadia MicroXCT-200 X-ray imaging system equipped with switchable scintillator-objective lens units. Tomographies were performed at either (i) 4× magnification, exposure time of 2 s, and calculated pixel size of 5.5 µm; or (ii) 10× magnification, exposure time of 8 s and calculated pixel sizes of 2.22 µm. X-ray source settings were 40 kV and 8 W resulting in 200 mA source current. Tomography projections were reconstructed using XMReconstructor software (Zeiss) yielding image stacks in TIFF format. All scans were performed using Binning 2 (summarizing 4 pixels), resulting in noise reduction and subsequently reconstructed using Binning 1 (full resolution) to avoid information loss. Anatomical structures were then visualized by manual and automated segmentation and 3D visualization using ITK-Snap 3.2.036.

RNA sequencing and transcriptomics

28.3 mg of scolus tissue was cut from a single newly-molted last instar caterpillar of unknown sex and stored in 1 mL RNAlater (#AM7020, Thermo Fisher, Waltham, MA, USA) at –80°C. To extract RNA, tissue was transferred to 0.5 mL TRIzol reagent (#15-596-018, Invitrogen, Carlsbad, CA, USA) and homogenized with a THq digital homogenizer (Omni International, Kinnesaw, GA, USA) for 30 s, and allowed to stand at room temperature for 5 min. After addition of 100 µL chloroform, the sample was shaken and allowed to stand at room temperature for a further 5 min, then centrifuged at 12,000 *g* at 4°C for 10 min. The upper aqueous phase containing RNA was removed with a pipette to another RNAse-free 1.5 mL tube. After addition of 250 µL of ice-cold 2-propanol to precipitate RNA, the sample was vortexed to mix, allowed to

stand 5 min at room temperature, and centrifuged again at 12,000 *g* at 4°C for 10 min. The supernatant was removed, and 500 µL ice-cold 75% ethanol was added to wash the pellet, before centrifuging again at 12,000 *g* at 4°C for 10 min. The supernatant was removed and the pellet allowed to partially air-dry before resuspending in RNAse-free ultrapure water. RNA concentration and purity was estimated using a Nanodrop spectrophotometer (Thermo Fisher). PolyA$^+$ RNA isolation, TruSeq stranded mRNA library construction, and nucleotide sequencing on an Illumina NextSeq 500 instrument were performed at the Institute for Molecular Bioscience Sequencing Facility.

Sequencing reads were assembled into contigs using Trinity 2.2.0 (1) and CLC Genomics Workbench 8.0.2, then sequences were trimmed with default settings on Trimmomatic and assembled using default parameters. For assembly with CLC Genomics Workbench, reads were trimmed to a quality rate of 0.01 with maximum ambiguous bases = 2, and four assemblies produced using a k-mer length of 31, 42, 53, and 64. To produce a database for MS-based protein identification, these five assemblies containing a total of 1,312,527 contigs were pooled into a single file, and ORFs encoding polypeptides larger than 25 amino acid residues were extracted using TransDecoder. After removing redundant sequences using CD-HIT, with identity threshold 100% and word size 8, a total of 1,324,013 possible amino acid sequences remained. These sequences were used as a database for MS identification of proteins, together with a database of 159 common MS contaminants. The abundance of each transcript encoding an identified venom polypeptide was calculated by mapping the raw reads to venom-encoding contigs using Geneious with options 'map randomly' and identity threshold of 95%. The raw sequencing reads used in this project are available from the National Centre for Biotechnology (NCBI)'s Sequence Read Archive in fastq format under BioProject ID PRJNA672259. The assembled contigs are available from the Transcriptome Shotgun Assembly archive, accession GIWX00000000.

Proteomics

For MALDI-TOF MS, 0.4 µL of venom or reconstituted HPLC fraction was spotted together with 0.4 µL α-cyanohydroxycinnamic acid (CHCA) and allowed to dry, then analyzed using a SCIEX 5800 MALDI-TOF MS with laser power 3,000–5,000. The *m*/*z* range was 100–1,000 or 1,000–7,000 for reflectron-positive mode and 2,000–25,000 for linear mode measurements.

For LC-MS/MS, whole venom samples and reconstituted HPLC fractions were analyzed on SCIEX 5600 and 6600 model triple-TOF MS instruments coupled to LC systems. For whole venom, approximately 50 µg dry weight of venom (estimated using A_{280} measured on a Nanodrop spectrophotometer) was used per sample. For HPLC fractions, 1/10th of the entire fraction was used. Reduced, alkylated and trypsinized samples were prepared by diluting the sample to be analyzed in reducing/alkylating solution (1% 2-iodoethanol, 0.25% triethylphosphine, 48.75% acetonitrile (ACN), 50 mM ammonium carbonate at pH 11.0) and incubating the sample for 1 h at 37°C. Samples were then dried by vacuum centrifugation and reconstituted in digestion reagent (20 ng/µL sequencing-grade trypsin (#7575, Sigma Aldrich, St Louis, MO, USA) in 40 mM ammonium bicarbonate pH 8.0, 10% ACN) before quenching in an extraction reagent (50% ACN, 5% formic acid (FA)), vacuum centrifugation, and reconstitution in 1% FA. Reduced and alkylated (but not trypsinized) and native MS samples were generated by omitting the digestion step, or the reduction, alkylation, and digestion steps in the above protocol, respectively.

The 5600 MS instrument was equipped with a Turbo V ion source and coupled to a Nexera X2 LC system (Shimadzu, Kyoto, Japan) equipped with a Zorbax 300SB-C18 column (#858750–902, Agilent, Santa Clara, CA, USA) incubated at 60°C. Peptides were eluted over 75 min using a gradient of 1–40% solvent B (90% ACN/ 0.1% FA) in solvent A (0.1% FA) at a flow rate of 0.2 mL/min. MS^1 scans were collected between 350 and 2200 m/z, and precursor ions in the range *m*/*z* 350–1500 with a charge from +2 to +5 and signal >100 counts/s were selected for analysis, excluding isotopes within 2 Da. MS/MS scans were acquired with an accumulation time of 250 ms and cycle time of 4 s. The 'Rolling collision energy' option was selected in Analyst software, allowing collision energy to be varied dynamically based on *m*/*z* and *z* of the precursor ion. Up to 20 similar MS/MS spectra over *m*/*z* range 80–1500 were pooled from precursor ions differing by <0.1 Da. The same settings were employed for the 6600 MS instrument, except it was coupled to an Eksigent LC system with a ChromXP-C18−CL column (150 mm × 0.3 mm, 3 µm; Eksigent, Livermore, CA, USA) run at a flow rate of 5 µL/min. Some samples were analyzed with focus on non-polypeptide toxins

using the 5600 MS instrument. For these LC-MS/MS experiments, the parameters were the same except that the m/z range was set to 80–1,000 for MS^1 scans.

The resulting spectral data in WIFF format were then compared with the amino acid sequence database described in Section 5.4 using the Paragon 4.0.0.0 algorithm implemented in ProteinPilot 4.0.8085 software (SCIEX, Framingham, MA, USA). Four different samples of reduced, alkylated, and trypsinized venom analyzed on the 5600 MS instrument were combined in a single search; the other three searches (reduced, alkylated, and trypsinized) on the 6600 MS; and reduced and alkylated on 5600 MS and on 6600 MS represent spectral data from a single LC-MS/MS analysis of one sample of pooled venom. A mass tolerance of 50 mDa was used for both precursor and MS/MS ions. Low-quality identifications (<95% confidence at the protein level, or <2 tryptic fragments detected with >95% confidence) along with contaminant and decoy database identifications were removed, then the remaining identifications from the four Paragon searches were pooled to form a draft venom proteome.

The contigs encoding polypeptides in the draft proteome were checked for quality by mapping the raw sequencing reads against them in Geneious Prime 2019.0.4, and analyzing each ORF manually for sequence variants and completeness. The updated ORFs were then translated, and the resulting amino acid sequences, including multiple variants, added to the draft proteome. This draft proteome was then analyzed using the Paragon and ProtGroup algorithms, and sequence variants whose identification was not supported by spectral data were removed. The spectral data for each identified polypeptide sequence was then analyzed with respect to the likely mature form of the protein, including N- and C-termini and the presence of PTMs. Spectral data were reviewed manually using Analyst 6.1 and PeakView software. For each identified precursor sequence, minor proteoforms with <10% of the maximal MS^1 spectral counts for each amino acid sequence were removed, and the proteoform with maximal MS^1 spectral counts called the 'mature form'. MS data were submitted to the ProteomeXchange Consortium via the PRIDE partner repository with the dataset identifier PXD022400.

Each precursor sequence was annotated for a secretion signal sequence using SignalP 4.1 (2), for homology to known sequences using BLAST searches against the Swiss-Prot and UniRef90 online databases, and HMMER searches (3) against the Pfam database. Polypeptide precursors were grouped by BLAST searches against each other (threshold E < 0.001). The final determined proteome, comprising 151 amino acid sequences and the ORFs that encode them, were submitted to NCBI where they were assigned GenBank Accession numbers of MW182018–MW182168.

Calcium imaging of DRGs

DRG from 4 week old male C57BL/6 mice were dissociated and plated in DMEM (Invitrogen, Carlsbad, California, USA) containing 10% fetal bovine serum (FBS, Assaymatrix, Melbourne, VIC, Australia), and penicillin/streptomycin (Gibco, Carlsbad, CA, USA) on a 96-well poly-D-lysine-coated culture plate (Corning, New York, NY, USA) and maintained overnight. Cells were loaded with Fluo-4 AM calcium indicator according to the manufacturer's instructions (Thermo Fisher Scientific). After loading (30 min at 37°C then 30 min at 23°C), the dye-containing solution was replaced with assay solution (Hanks' balanced salt solution, 20 mM HEPES). Fluorescence corresponding to $[Ca^{2+}]_i$ of 100–150 DRG cells was monitored in parallel using a Ti-E deconvolution inverted microscope (Nikon, Tokyo, Japan), equipped with a Lumencor Spectra LED lightsource. Images were acquired with a 20× objective at one frame per second (excitation 485 nm, emission 521 nm). Baseline fluorescence was monitored for 30 s. At 30 s, assay solution was replaced with assay solution (negative control), and at 60 s with venom (50 ng/µL) in assay solution or reconstituted HPLC fraction (1/10th of total fraction). Experiments involving the use of mouse tissue were approved by The University of Queensland Animal Ethics Committee (TRI/IMB/093/17).

Solid phase peptide synthesis

Peptides were assembled by solid-phase peptide synthesis using an automated microwave Liberty Prime synthesizer (CEM, Charlotte, NC, USA) at a 0.1 mmol scale with Fmoc chemistry. Polystyrene Rink-amide resin was used for C-terminally amidated peptides or polystyrene Wang resin with the appropriate C-terminal residue was used. Couplings were performed in dimethylformamide (DMF) using 5 eq of Fmoc-protected amino acid/0.25 M Oxyma Pure/2 M *N*,*N*′-diisopropylcarbodiimide, relative to resin substitution,

for 1 min at 105°C. Fmoc removal was accomplished by treatment with 25% pyrrolidine/DMF (40 s at 100°C). Side-chain protecting groups used were Arg-Pbf, Lys-Boc, Ser/Tyr-tBu, Asn/His-Trt, and Glu-OtBu. Cleavage and simultaneous removal of side-chain protecting groups were carried out using a CEM Razor rapid peptide cleavage system for 30–60 min at 40–45°C in cleavage solution (92.5% TFA, 2.5% triisopropylsilane, 2.5% H_2O, 2.5% anisole or 3,6-dioxa-1,8-octanedithiol). Following filtration of cleavage solution, ice-cold diethyl ether was added to precipitate crude peptides. Crude peptides were washed with diethyl ether and centrifuged three times (6000 *g*, 5 min), then resuspended in 0.1% TFA/50% ACN/H_2O, filtered, and lyophilized. Peptides were purified by preparative RP-HPLC on a Waters 600 or Shimadzu Prominence HPLC system using a Zorbax 300SB C18 column (21.2 × 100 mm; Agilent, Santa Clara, CA, USA) using a 0–60% gradient of solvent B (90% ACN, 0.045% TFA) over 60 min at a flow rate 8 mL/min, with monitoring at 214 and 280 nm. Fractions were collected using a FC-10A fraction collector and mass and purity confirmed using ESI-MS and UPLC in addition to LC-MS. For cysteine-containing peptides, air oxidation was performed in 0.1 M NH_4HCO_3 (pH 8.2) for 2 days to allow formation of disulfide bonds.

Recombinant expression

Larger disulfide-rich peptides were produced using an *Escherichia coli* periplasmic expression system optimized for production of cystine-rich venom peptides (4). In this system, the peptide is produced as a fusion protein with MalE signal sequence for periplasmic export, N-terminal His_6 tag for affinity purification, maltose binding protein (MBP) to enhance solubility, followed by a tobacco etch virus (TEV) protease cleavage site preceding the desired peptide sequence. Plasmids with codons optimized for high-level expression in *E. coli* were produced by GeneArt (Regensburg, Germany) and transformed into the protease-deficient *E. coli* strain BL21-λDE3.

To optimize expression conditions for each construct, a 5 mL culture in LB medium with 100 µg/mL ampicillin was inoculated with 5 µL glycerol stock and grown for 16 h at 30°C with shaking at 180 rpm. 250 µL of this overnight culture was used to inoculate 5 mL cultures containing either LB, terrific broth (TB), or ZYP-5052 (5) medium (ZY) supplemented with ampicillin (100 µg/mL). These cultures were grown at 24°C, 180 rpm until the LB culture reached an OD_{600} of 0.8–1.0, then the culture was cooled to 16°C over 30 min. The LB and TB cultures were then induced by addition of 1 µM isopropyl-β-D-thiogalactoside (IPTG), and expression allowed to proceed for 20 h at 16°C. Fusion protein expression was evaluated by SDS-PAGE after lysis at 37°C for 30 min in 240 µL 2 mg/mL lysozyme (#L6876, Sigma Aldrich).

For large-scale expression, a 300 mL culture of LB with 100 µg/mL ampicillin was inoculated with 5 µL glycerol stock and grown for 16 h at 30°C with shaking at 180 rpm. 50 mL of this overnight culture was used to inoculate six cultures each containing 1 L of the optimal medium supplemented with 100 µg/mL ampicillin and 100 µL antifoam (#A8582, Sigma Aldrich) in a 5 L baffled flask. Cultures were grown at 24°C with 300 rpm shaking until OD_{600} 0.8–1.0, then the cultures were cooled to 16°C over 45 min. LB and TB cultures were induced with 1 µM IPTG, whereas ZY cultures were left to auto-induce. Expression was allowed to proceed over 16 h at 16°C with shaking at 300 rpm. Cells were harvested by centrifugation (6,000 *g*, 4°C, 20 min), resuspended in 20 mL per g pellet weight of TN buffer (400 mM NaCl, 20 mM Tris-Cl pH 7.5) supplemented with 15 mM imidazole. Cells were lysed using a constant pressure cell disruptor at 32 kpsi, 4°C and the lysate clarified by centrifugation (18,500 *g*, 4°C, 30 min). Clarified lysate corresponding to each liter of expression culture was applied to 5 mL HisPur Ni-NTA beads (#88832, Thermo Fisher) saturated with Ni^{2+} and the fusion protein eluted with 20 mL TN buffer containing 500 mM imidazole. The eluant was concentrated to 5 mL using a 30 kDa cut-off centrifugal concentrator (#UFC903024, Merck Millipore, Burlington, MA, USA), diluted to 15 mL to reduce the imidazole concentration, then re-concentrated to 5 mL. The concentrated fusion protein was then mixed with 5 mL of 2× cleavage buffer (10 mL TN buffer, 1.8 mg reduced glutathione, 3.6 mg oxidized glutathione, 500 µL 1 mg/mL recombinant TEV protease) and the sample incubated for 40 h at room temperature on a roller. The released MBP was then precipitated by addition of 100 µL TFA and precipitate removed by centrifugation (18,000 *g*, 4°C, 10 min). The released peptide was then purified on a Shimadzu LC system with a C4 RP-HPLC column (10 × 250 mm; #00G-4168-N0, Phenomenex, Torrance, CA, USA) employing a gradient of 5–65% solvent B (90% ACN, 0.43% TFA) in solvent A (0.5% TFA) over 45 min at a flow rate of 5 mL/min. Fractions were screened using MALDI-TOF MS and peptides matching the expected mass lyophilized and further purified via RP-HPLC using a C18 RP-HPLC column (4.6 × 250 mm; #00G-4482-E0, Phenomenex). Peptides were lyophilized and

reconstituted in ultrapure water, then concentration estimated using A_{280} measured on a Nanodrop spectrophotometer together with the peptide's extinction co-efficient calculated using ProtParam (https://web.expasy.org/protparam/). Peptides were diluted in ultrapure water to a concentration of 5 mg/mL and stored at –20°C.

ACPR functional activation assay

We used previously described plasmids for expression of *A. aegypti* GnRH-related receptors, namely ACPR, AKHR-IA and CRZR, in mammalian cells (6, 7). Chinese hamster ovary (CHO) K1-aeq cells (8), which stably express the calcium-dependent bioluminescent protein aequorin, were grown and transfected with plasmid as described (6). Two days after transfection, cells were detached using Dulbecco's PBS (Wisent, St. Bruno, Quebec, Canada) containing 5 mM EDTA, and then prepared for functional assays as described (9). Various concentrations (10 pM to 1 µM) of synthetic *A. aegypti* GnRH-related neuropeptides (ACP, AKH, and corazonin) and three *D. vulnerans* Family 1 venom peptides (U-LCTX$_1$-Dv1, -Dv4, and -Dv5) were prepared in assay medium (as previously described (9)) and loaded into 96-well white luminescence plates (Greiner Bio-One, Kremsmünster, Austria) in quadruplicate. Transfected CHO K1-aeq cells were automatically injected into each well of the 96-well plates containing different neuropeptides or venom peptides along with negative and positive control treatments as described (9). Kinetic luminescent response of cells expressing the *A. aegypti* GnRH-related receptors was measured for 20 s immediately after injection of cells into each well containing the different treatments using a Synergy 2 Multi-Mode Microplate Reader (BioTek, Winooski, VT, USA).

In vivo *assays*

The toxicity of venom and venom peptides was evaluated by injection into female fruit flies (*D. melanogaster*) 4–6 days post-emergence. Female flies were used to reduce variability, and because their larger size facilitates injection. Groups of eight female flies were assayed in triplicate for each dose tested. Injection needles were formed by pulling glass capillary tubes (#3-000-203-G/X, Drummond, Birmingham, AL, USA) on a micropipette puller (Model P-97, Sutter Instrument Co., Novato, CA, USA) and trimming the fine tip manually using tweezers. Needles then were filled with mineral oil, connected to a Nanoliter 2000 microinjector (Kanetec, Bensenville, IL, USA) equipped with a foot pedal, and ~1 µL of venom (~1 mg/mL) or peptide (1 mM) aspirated. Each group of flies were immobilized by cooling the 5 mL tube in which they were contained for ~2 min on ice, and then decanted on top of the 'injection stage', a petri dish filled with ice. Under a dissecting microscope, each fly was carefully impaled on the lateral thorax behind the wing, and 50.6 nL of diluted venom or water was injected. Subsequent to injection, each group of flies were returned to their 5 mL plastic tube at room temperature and their behaviour observed.

Crickets were purchased from Pisces Live Food (Brookfield, QLD, Australia), and water or peptide (1 mM) injected into the thorax using a 1 mL syringe driven by a hand microapplicator (Burkard Scientific, Uxbridge, UK). After injection, individual crickets were placed in a 60 × 15 mm plastic petri dish for observation.

For mouse behavioral experiments, peptide (600 pM in 20 µL saline containing 0.1% BSA) was administered to male adult (12 to 15 weeks old) C57BL/6J mice by shallow intraplantar injection into the hindpaw. Three mice were injected per peptide. Following injection, spontaneous pain behavior events were counted from video recordings. All mice were acclimatized before experiments, and all measurements were performed by a blinded observer. Experiments involving animals were approved by The University of Queensland Animal Ethics Committee (PHARM/526/18).

H. contortus larval development assay

Peptides were prepared as detailed previously and prepared as five-fold serial dilutions in distilled water. Technical grade levamisole was purchased from Sigma and the commercial drench product Zolvix® was used for monepantel. Both were dissolved in dimethyl sulfoxide (DMSO) at 10 mg/mL, and serially diluted 2-fold to give a series of working concentrations.

H. contortus eggs were isolated as described previously (10) from the feces of sheep infected with either the *Hc* Kirby isolate, which is susceptible to all commercial anthelmintics, or the *Hc* MPL-R multi-drug

resistant isolate (11) that is resistant to all major anthelmintic classes. Larval development assays were conducted in 96-well microtiter plates as described (10). For peptide assays, each well contained 50 µL of 2% agar, 20 µL egg solution, and 20 µL peptide solution (or water for negative control). For commercial anthelmintics, each well contained 200 µL of 2% agar and 2.0 µL of anthelmintic in two-fold dilutions in DMSO (controls contained DMSO only). Plates were incubated at 26ºC for six days and then larvae were killed and stained with Lugol's iodine solution. The number of larvae that had developed to the infectious third-larval stage were counted and expressed as a percentage of controls. For dose-response experiments, duplicate assays were performed three times for peptides and twice for commercial anthelmintics. Median inhibitory concentration (IC_{50} values) and 95% confidence intervals (95% CI) were calculated using non-linear regression in GraphPad Prism v8. All animal procedures were approved by the University of New England Animal Ethics Committee (Approval number AEC18-033).

Statistical analysis

Dose-response curves for insecticidal, nematocidal, and receptor activation assays were fitted as four-parameter Hill equations in GraphPad Prism 7.02 or 8.0 (GraphPad Software, San Diego, CA, USA) or IgorPro 6.4 (Wavemetrics, Lake Oswego, OR, USA). For DRG assays, median F/F_0 values ± interquartile ranges are shown, and conditions were compared using the non-parametric Kruskal-Wallis test. For *in vivo* pain assays, the time during which animals displayed nocifensive behaviors over 2-min bins was compared to vehicle injections using an unpaired Student's *t*-test.

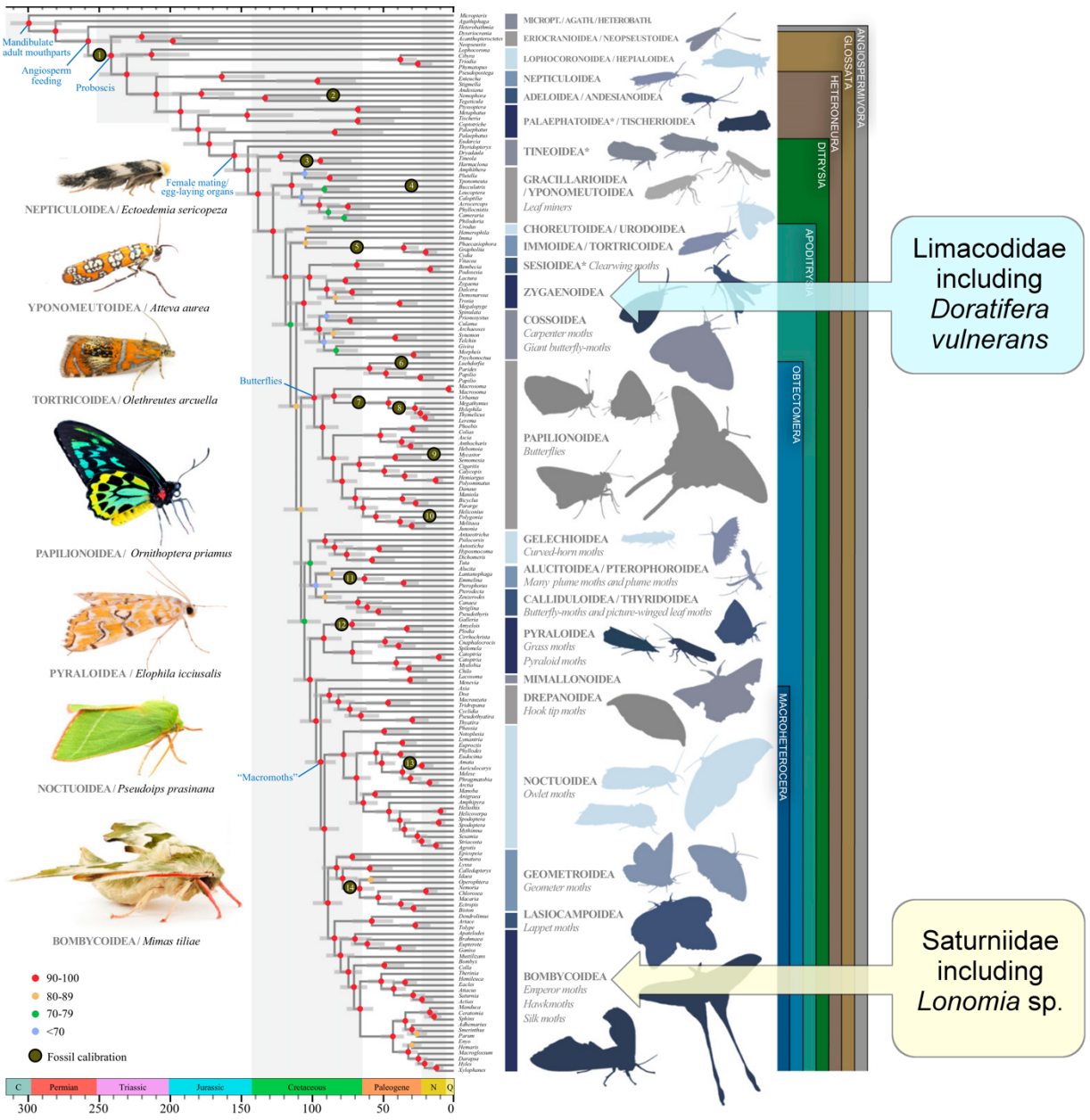

Fig. S1: Multiple independent origins of venom use in Lepidoptera. From Kawahara et al. (12), with phylogenetic positions of venomous limacodid and saturniid caterpillars marked.

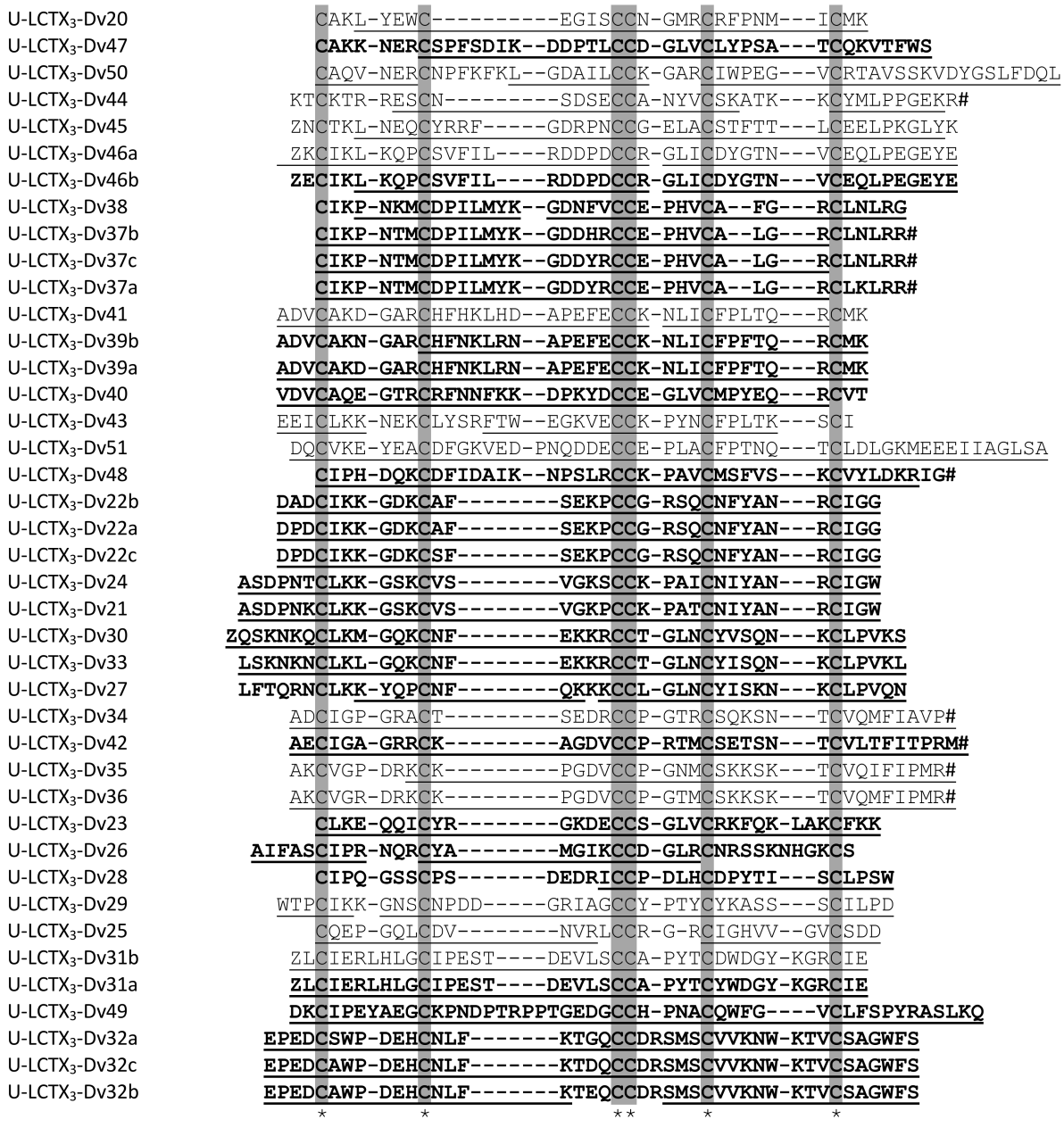

Fig. S2: Alignment of inhibitor-cystine-knot-like venom peptides (Family 3). Cysteine residues are highlighted in grey. Peptides detected in intact untrypsinized form with high confidence are shown in **bold**. Tryptic fragments detected with high confidence are underlined. Z, pyroglutamic acid; #, C-terminal amidation.

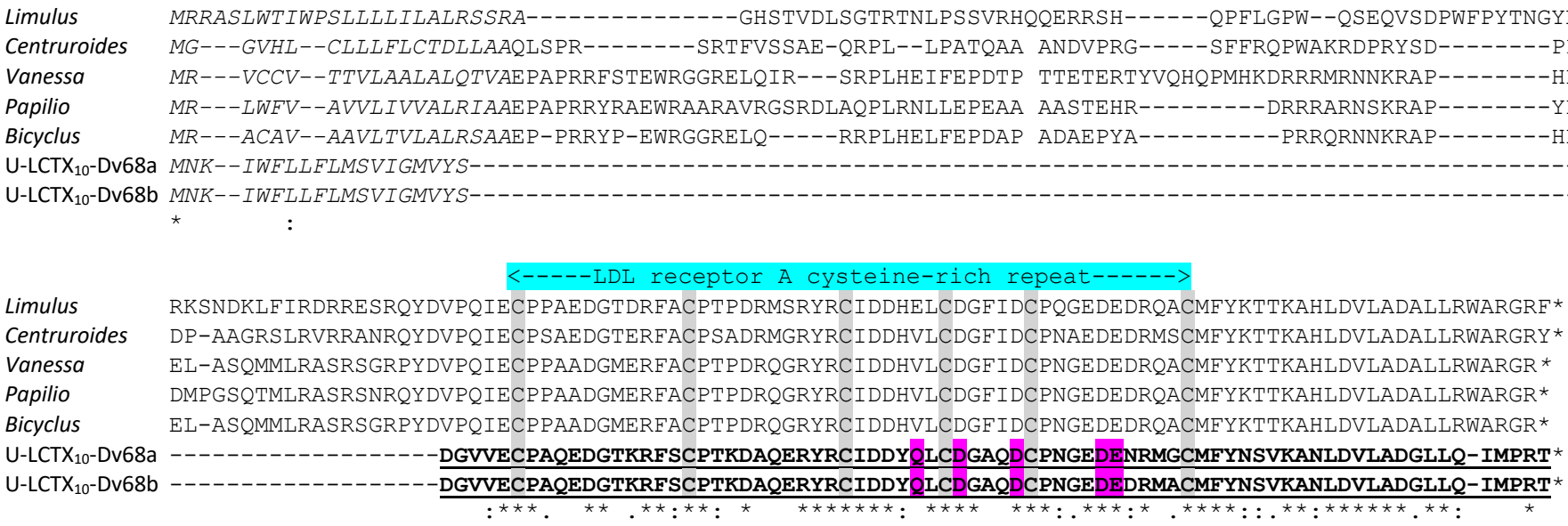

Fig. S3A: Alignment of Family 10 venom peptides with most similar sequences retrieved by BLAST search against the NCBI non-redundant protein sequence database. All comparison sequences represent uncharacterized polypeptides similar to the low-density lipoprotein (LDL) receptor A cysteine-rich repeat domain (marked by dark blue bar). Cysteine residues are highlight in grey. Predicted signal sequences are shown in *italics*. Putative mature forms of Dv68a and Dv68b are shown in **bold**. Tryptic fragments detected with high confidence (>95%) in venom are underlined. Putative calcium-binding residues (13) are highlighted in magenta. Symbols below the sequence alignment indicate similarity in ClustalW format. *Limulus*, horseshoe crab *Limulus polyphemus* XP_022237332.1; *Centruroides*, Arizona bark scorpion *Centruroides sculpturatus* XP_023231755.1; *Vanessa*, Kamehamaha butterfly *Vanessa tameamea* XP_026498635.1; *Papilio*, common mormon butterfly *Papilio polytes* XP_013138063.1; *Bicyclus*, squinting bush brown butterfly *Bicyclus anynana* XP_023934104.1.

Fig. S3B (next page): Alignment of Family 19 venom peptides with homologous heteropteran venom protein family 3 and asilid venom protein family 11. Symbols underneath the sequence alignment indicate similarity in ClustalW format. Stars at the end of sequences represent stop codons. Pr, assassin bug *Platymeris rhadamanthus*. Pp, assassin bug *Pristhesancus plagipennis*. Pr_fam3_p1, *P. rhadamanthus* venom protein family 3 protein 1. ASTX, asilitoxin or asilidin. Dg, robber fly *Dolopus genitalis*.

```
U-LCTX19-Dv83       MR--------AVTIILLLSLCSVSY----------------------------------------------------SQSHDLVLGRALPGDLILYKVNEWK--YGFPLLVRTSVIEYP
U-LCTX19-Dv84       MR--------ALTVILLFSICSACH----------------------------------------------------SQSHDVTLGRAQPGDVLLYKGEEWK--YGFPLFIRTTLFEFP
U-LCTX19-Dv85       MR--------VTLKILVFCLCSVNY----------------------------------------------------SMTHDLVVGRALPSDILLYKVNEWK--RGFPLMVRSSTIKYP
U-LCTX19-Dv86       MRT-------LKFIILVCSLYTANCSE---------------------------------------------DTVKPV-FESHDLILGKAMSGDTLLLTSTEKK--IGFPLIKRTSEIVFP
U-LCTX19-Dv87       MRA-------VVSLILFVYFCTSSHSKSL-------------------------------------------TSSHSK-SLSHNLYAGQPHPTEILVFETTQAK--IGVPLTIRKTIIKFP
Pr_fam3_p1          MTSF-----SALLVALLVTVTVPNSA-----------------------------------------------FAINCAIGQNHSASFGSRTPGDKLVFQNHIQR--AWKKFEYTKVVVTYP
Pr_fam3_p2          MKSLKSIFYWTSLAILLAIFIAPSPV-----------------------------------------------LTGKCS-GKSHNATFGSKRPGDKLLFKDHIVE--KWRFLGFARREIIFP
Pp_fam3_p1          MSLIRGLFCSTFLVAVIIIITAPNLS-----------------------------------------------SAAKCP-GVKHNLIVGTRLHKDMLLSKEHIQS--SWKLIGTVKKTITYP
U-ASTX11-Dg36       MNNF------VTVLLMVIGSLVNNV-----------------------------------------------------YSQNNIIWGAVGPNDVHLFRERVIE--PIRHNQVVTKNVLYP
U-ASTX11-Dg32       MKYF------MVFAFAIIACLSA-------------------------------------------------------VSASNSTFGAISPSDSKLHEENVFK--SASPLRIVTKDVKFG
U-ASTX11-Dg13       MKYF------GILALALVA-CVAVSN-----------------------------------------------------AQSNNMSWGSIGPGDSLLDRQIISK--PSKWLRIVTQDYTFP
U-ASTX11-Dg7        MKYF------GILALALAA-CVVITN-----------------------------------------------------AQSHNSLWGSIGPGDNLLDRQIIKK--SYKFLRIVTQDYTFP
U-ASTX11-Dg1        MKSF------GVLALLVIAACVAESY-----------------------------------------------------AQSHNVVFGSIQPGDRKLFQQIVMK--KAKTLRVVSEDVQYP
U-ASTX11-Dg15       MRHL------IVVILAVIGICFFSVS-----------------------------------------------------AQKHSVTFGKAGPEDRLLYSTLVKR--PAKKGWEVSENVFYP
Pp_fam3_p2          MAKI------AVFTLLLVCFCSTLGW-----------------------------------------------AQYRN-NGTHNLIVGRRGYNDLILYERTVAKGKTWNPFGKVSEDVTYP
U-ASTX11-Dg30       MTALKIFICAAFWAVLSIQSADTSLIFRQIEDLETNNNTLDYSGVETIETHIQLIGEN QNEALDQTE--LT-QNV-GVTKYYSLGKRIAGDRVVATGGKAM--NWSTPHNVKITLAYP
U-ASTX11-Dg26       MYRTPCLVLLTLAAVFAFDLDTVQFRAQLLN-----------GDIVVVNETTRFQRKY PNVTLNGMM--LKTKLV-KGQINYQLGKRIPGDQLVAEKADKQ--SFPAPEDIQIVLRYP
U-ASTX11-Dg25       MARF----HITLACILLATACAAAPEHDQIG-----------LSVEVIDDITEYLAKY PESEITPLRVVVS-PIP-PFRTRYVLGTRVKGDRVLAIRNDNV--FYPTRRDIRLDLHYP
U-ASTX11-Dg24       MARF----NFALACILLAAVCSAAPEIEKLQ-----------ASIEFVDDISAYAAEF PEVDLIPLD--SE-VQP-FGQIRYTLGGRVAGDRIVAQGNNNF--NYPTLQDVRLTLNYP
U-ASTX11-Dg22       MSRF----FITLACIAFVGVCSA----QNLD-----------QHVQFVEDIEKFRAEN PEVVLTPLT--VESVTP-YNQMRYTFGRRVLGDRIVTQGNNNF--NYPQAQDVRTNLNYP
U-ASTX11-Dg23       MARF-----IALACVLLAA-CAVASEFDQFD-----------STVEVVDNINTYLVDN PDAELIELQ--AQ-SMP-FAKTRYTFGQRVNGDRVLAQRNDNF--NYGRMQDVRLNLNYP
U-ASTX11-Dg20       MARF-----IALACLLLVAICAASPE---FE-----------SSIEVIDNIDTYLADN PDAELIALQ--VQ-SMP-FAKSRYSFGRRVPGDRILAKRNENS--NYARMQDVRINLNYP
                     *                                                                  *     :  :                     :

U-LCTX19-Dv83       --ELGQ-SNFAIITAIVIIDNNYDGHGGYPVVEAGGVGQDFVKIKLESERSYGFNFTITIYGRNR-----IFI*
U-LCTX19-Dv84       --KPNT-GNIAYISAIIIRDHYYDGTGGFASIKAGGVGQNFVKIELKSQRHHGFRFTISIYGQFLN---RMY*
U-LCTX19-Dv85       --ETKA-NNYVYISAIYVQDHYYYGHEGYPSIKSGGVGQSSVSIKLKTQRSHGMNFTIFIHGRYLN---GMY*
U-LCTX19-Dv86       --EPGK-ENFAHITAIVIKDKYTDGNGGLATILAGGLGKKFVKIKLATKRGHGFHFTVKIYGRN*
U-LCTX19-Dv87       --EEGK-KNDRFINNIIALDNIRDGKGGYASVIDGGVGQKHAKIKIESERSHGFNFTIRIYASK*
Pr_fam3_p1          --SEGE--TGQNISYIELTDKYTNGHGACPKILEGGVGTNNVRIELKSGFYRGIDFVVKIYSI*
Pr_fam3_p2          --LKGE-KRKYIITEIKLTDRYKNGHGGCPEIKEGGVNNDHVKINIKSEFTRGFDFDIEIYGLKKSKARKLKY*
Pp_fam3_p1          --RKKEDENKYIITQIKVLDKYTNGHGGCPSIRKGGVGHSNVTVLLEGEILRGLEFDVEIYGLKRSKAKKLFKLN*
U-ASTX11-Dg36       --PAGQ-SQDHTITAIVLTDVHTDGNGGYATLQSGGPGQTHATVHFVSALGHSVNYIMEVYGRRI*
U-ASTX11-Dg32       --YKGN---RKVITGIRVIDRMPKQKGGRASLLHGGPGHKNVTIHLKSQRNNGIFFTVEIYGR*
U-ASTX11-Dg13       --PPGS-VQNRLITGIRVTDQYTNGKGGYASLYAGGPGYNSVTIHLKSQRSQGFKFIVEIFGR*
U-ASTX11-Dg7        --PPGA-VLGRMITGIRVTDQYTNGKGGYASLYAGGPGNPSVTIHFKSQRNHGFNFIVEIFGR*
U-ASTX11-Dg1        --PKGV-VGQNLITGIRVTDQYTNGKGGYSTLVAGGPGQRDVTLHFKSQRGHGYNFIVEYYGR*
U-ASTX11-Dg15       GIGGGA-SYDHIFTEIRVTDKCEDGTGGYAYITEGGIGQRSAKIHFISQLSKGYEFLLEIFGH*
Pp_fam3_p2          VTYVPP-SMRRRITEIDAIDLIGNGKGGYAYITKGGINMSNVTIHFKSQSGKGYSFHLVIYGR*
U-ASTX11-Dg30       --TRGI---GALVTYVFIAVDQTN-NGGRAYVLNGGVNQRHITVVIEAFGVTHFALAASIYGR*
U-ASTX11-Dg26       --TKGE---GATVSHVNIVVDQSS-SVGDGYVIEGGISQKFIGILVEANNTMHFTFSASIYGYY*
U-ASTX11-Dg25       --QYGT---GGIVTLIDIAVEQSS-DLGRAYIVAGGIGQRQIKFVVEARDVYHLSTNTTIYGY*
U-ASTX11-Dg24       --QSGV---GAVVSFVEIVVQQTS-NDGNAYIAAGGIGQRTIRIILEARRTQSFAYRAAIFGY*
U-ASTX11-Dg22       --ANGI---GNVVSYVEIFVDQTS-NIGTAYVTSGGIGQRHISIVLEAKRTFRFSYRAAIYGY*
U-ASTX11-Dg23       --QWGV---GAIVTYLEVILEYNS-NMGKLYIVGGGIGQRSIKLVMEANGVTHFAASSTLWGY*
U-ASTX11-Dg20       --QSGV---GAVITHLDVNLEYDS-NMGKLVLIEGGIGRRTIKIAIEAKAVTHFAANVTLWGV*
                              .. :          .   :  ** .     . .            .
```

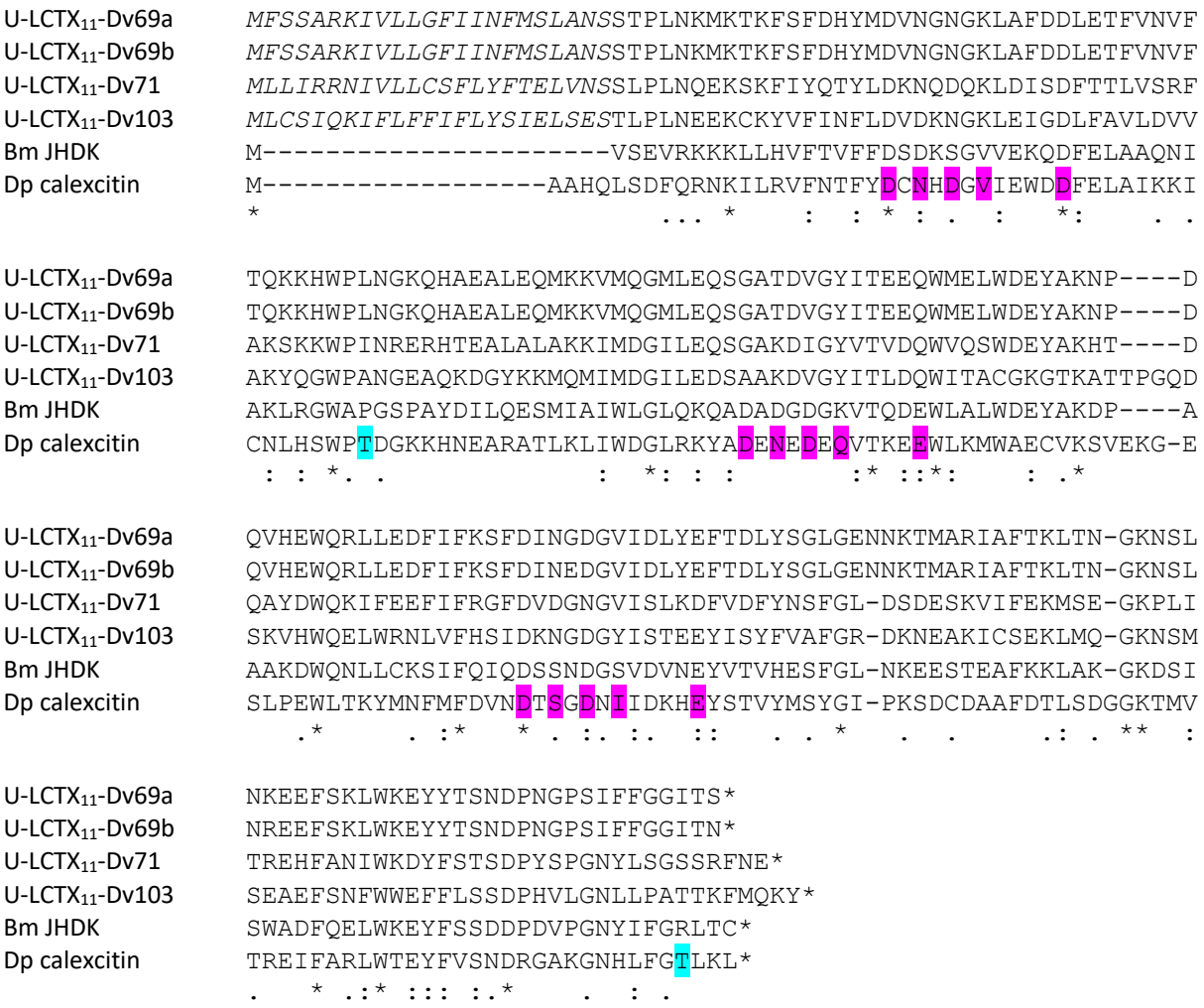

Fig. S3C: Alignment of Family 11 venom toxins with homologous sequences. Bm JHDK, silkworm *Bombyx mori* juvenile hormone diol kinase (14). Dp, squid calexcitin of *Doryteuthis* [formerly *Loligo*] *pealeii* (15). Predicted signal sequences are shown in italics. Calcium-binding residues in EF-hand motifs and phosphorylation sites of calexcitin are highlighted in magenta and light blue, respectively. Symbols underneath the sequence alignment indicate similarity in ClustalW format. Asterisks at the end of sequences represent stop codons.

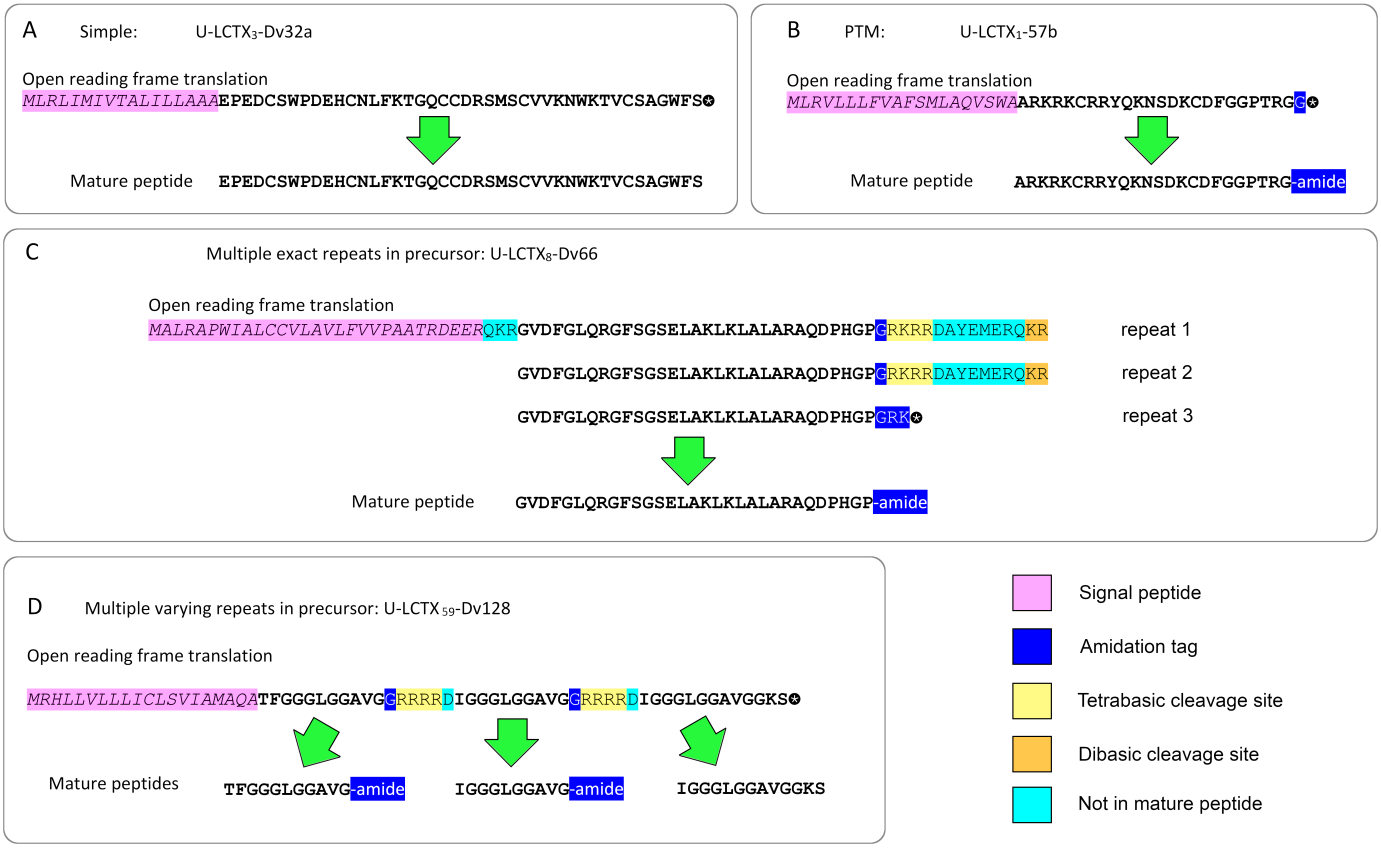

Fig. S4: Secretory processing of limacodid venom peptides. (**A**) Simple precursor with signal peptide (pink), mature peptide (bold), and stop codon (black circled star). (**B**) Precursor encoding PTM with signal peptide, mature peptide, and amidation tag (dark blue). (**C**) Precursor U-LCTX$_6$-Dv66, which encodes multiple copies of a diuretic hormone 31-like venom peptide, separated by amidation tags, tetrabasic cleavage sites (yellow), spacer regions (light blue), and dibasic cleavage sites (orange). (**D**) Precursor U-LCTX$_{59}$-Dv128, which encodes multiple variants of a glycine-rich peptide separated by tetrabasic cleavage sites.

Fig. S5A–L (next page): Heterologous expression of two disulfide-rich caterpillar toxins in *E. coli*. Panels on the left (A, C, E, F, I, J) show data for U-LCTX$_3$-Dv21. Panels on the right of the figure (B, D, G, H, K, L) show data for U-LCTX$_3$-Dv33. Panels A and B show SDS-PAGE analysis of samples collected during purification of a His$_6$-MBP-peptide fusion protein using nickel-NTA affinity chromatography. (**A**) Lane 1, HyperPage prestained protein ladder; lane 2, clarified cell lysate; lane 3, nickel-NTA column flow-through; lane 4, nickel-NTA elution; lane 5 and 6, fusion protein samples after cleavage by TEV protease at 4°C (lane 5) or 23°C (lane 6). Lanes in (**B**) are the same as in panel A except that lane 4 shows a pre-elution wash of the nickel-NTA column, and the column elution and cleavage reactions are shown in lanes 5–7. (**C–D**) RP-HPLC chromatogram showing purification of peptides after cleavage from the fusion proteins by TEV protease. Peaks for which the expected peptide masses were subsequently detected by MS are marked with a blue star. (**E–H**) Comparison of elution times of native (n) and recombinant (r) peptides using LC-MS. Blue traces show total ion chromatograms (TICs) of purified recombinant peptides. Black traces show the elution positions of the natural peptides, visualized as whole venom extracted ion chromatograms (XICs), using m/z values known to originate from the natural peptides (Dv21, 985.463 ± 0.1 Da; Dv33, 1115.072 ± 0.1 Da). Panels F and H show enlarged overlays for the data in panels E and G. Note that rDv33 differs from nDv33 by the presence of an N-terminal Gly residue but nevertheless elutes in almost exactly the same position. (**I–L**) MS of purified peptides prior to activity testing. For each assigned peak, the upper number shows the theoretical m/z value in Da, and the lower number shows the observed value. Panels I and K show average masses. Panels J and L show the monoisotopic masses as determined by examination of the M+4H$^+$ ion.

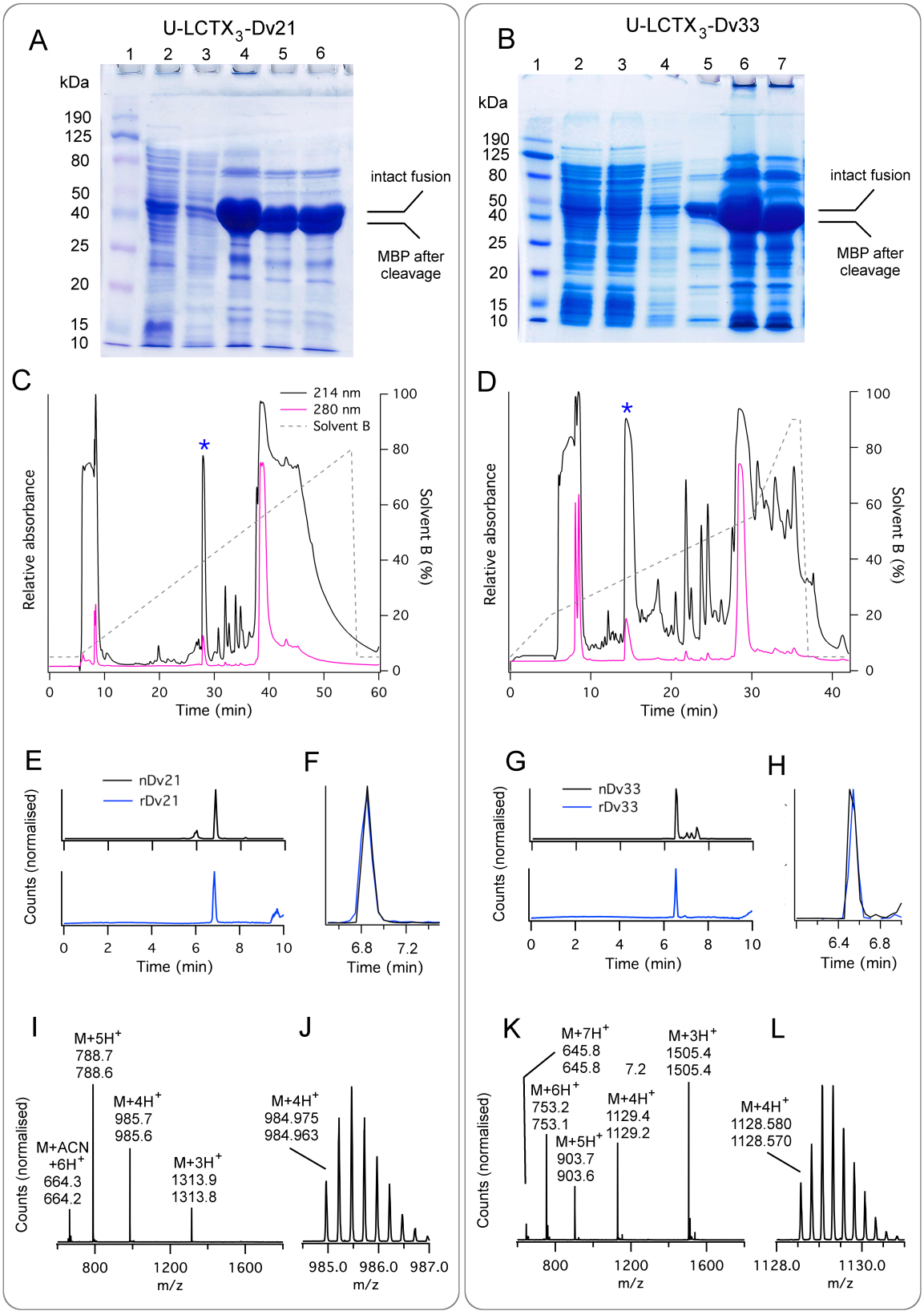
A
U-LCTX3-Dv21
1 2 3 4 5 6
kDa
190
125
80
50
40
25
20
15
10
intact fusion
MBP after cleavage
B
U-LCTX3-Dv33
1 2 3 4 5 6 7
kDa
190
125
80
50
40
25
20
15
10
intact fusion
MBP after cleavage
C
214 nm
280 nm
Solvent B
Relative absorbance
Solvent B (%)
Time (min)
D
Relative absorbance
Solvent B (%)
Time (min)
E
nDv21
rDv21
Counts (normalised)
Time (min)
F
Time (min)
G
nDv33
rDv33
Counts (normalised)
Time (min)
H
Time (min)
I
M+5H+
788.7
788.6
M+4H+
985.7
985.6
M+ACN
+6H+
664.3
664.2
M+3H+
1313.9
1313.8
Counts (normalised)
m/z
J
M+4H+
984.975
984.963
m/z
K
M+7H+
645.8
645.8
M+6H+
753.2
753.1
M+5H+
903.7
903.6
7.2
M+4H+
1129.4
1129.2
M+3H+
1505.4
1505.4
Counts (normalised)
m/z
L
M+4H+
1128.580
1128.570
m/z

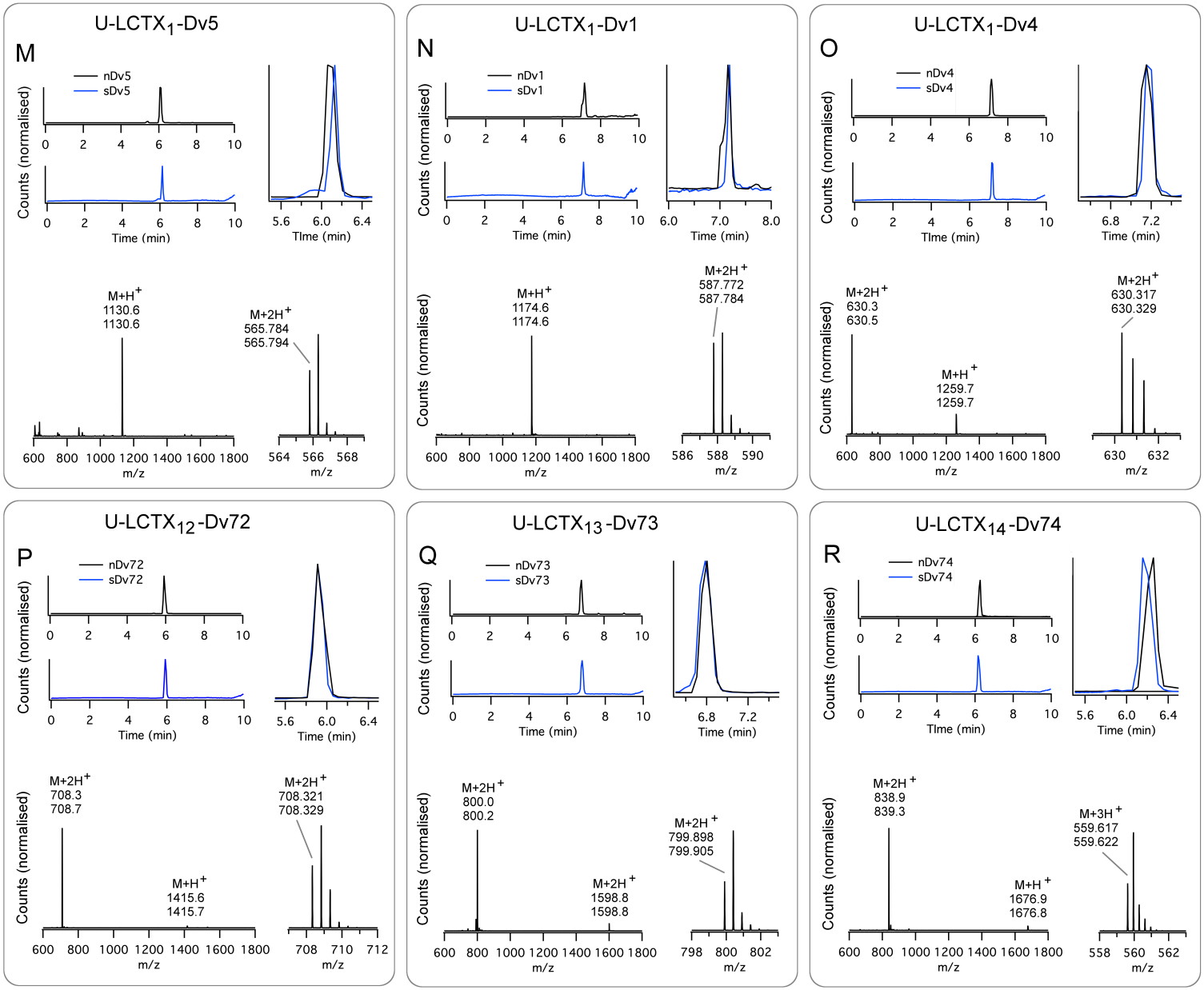
U-LCTX1-Dv5
M
nDv5
sDv5
Counts (normalised)
Time (min)
TIme (min)
M+H+
1130.6
1130.6
M+2H+
565.784
565.794
m/z
U-LCTX1-Dv1
N
nDv1
sDv1
M+H+
1174.6
1174.6
M+2H+
587.772
587.784
U-LCTX1-Dv4
O
nDv4
sDv4
M+2H+
630.3
630.5
M+H+
1259.7
1259.7
M+2H+
630.317
630.329
U-LCTX12-Dv72
P
nDv72
sDv72
M+2H+
708.3
708.7
M+H+
1415.6
1415.7
M+2H+
708.321
708.329
U-LCTX13-Dv73
Q
nDv73
sDv73
M+2H+
800.0
800.2
M+2H+
1598.8
1598.8
M+2H+
799.898
799.905
U-LCTX14-Dv74
R
nDv74
sDv74
M+2H+
838.9
839.3
M+H+
1676.9
1676.8
M+3H+
559.617
559.622

Fig. S5M–R (previous page): Production of synthetic venom peptides <2 kDa using solid-phase peptide synthesis. For each peptide, four panels are shown. The upper left traces show a comparison of the LC-MS elution times of the native peptide (black) visualized as an extracted ion chromatogram (XIC) of a prominent ion originating from the peptide ± 0.1 kDa; and the synthetic peptide (black trace) visualized using a total ion chromatogram (TIC). The upper right panel shows an overlay of the data in the first panel. In the lower panels, upper numbers show expected ion m/z values in Da and lower numbers show observed ion m/z values in Da. The lower left graph shows average masses from a low-resolution LC-MS, indicating peptide purity. The lower right panel shows the monoisotopic ion mass determined using high-resolution LC-MS indicating correct mass. (**M**) U-LCTX$_1$-Dv5; (**N**) U-LCTX$_1$-Dv1; (**O**) U-LCTX$_1$-Dv4; (**P**) U-LCTX$_{12}$-Dv72; (**Q**) U-LCTX$_{13}$-Dv73; (**R**) U-LCTX$_{14}$-Dv74.

Fig. S5S–W (next page): Production of synthetic venom peptides >2 kDa using solid-phase peptide synthesis. Format as in S4B. (**S**) U-LCTX$_7$-Dv63; (**T**) U-LCTX$_6$-Dv61; (**U**) U-LCTX$_8$-Dv66; (**V**) U-LCTX$_2$-Dv11; (**W**) U-LCTX$_2$-Dv12.

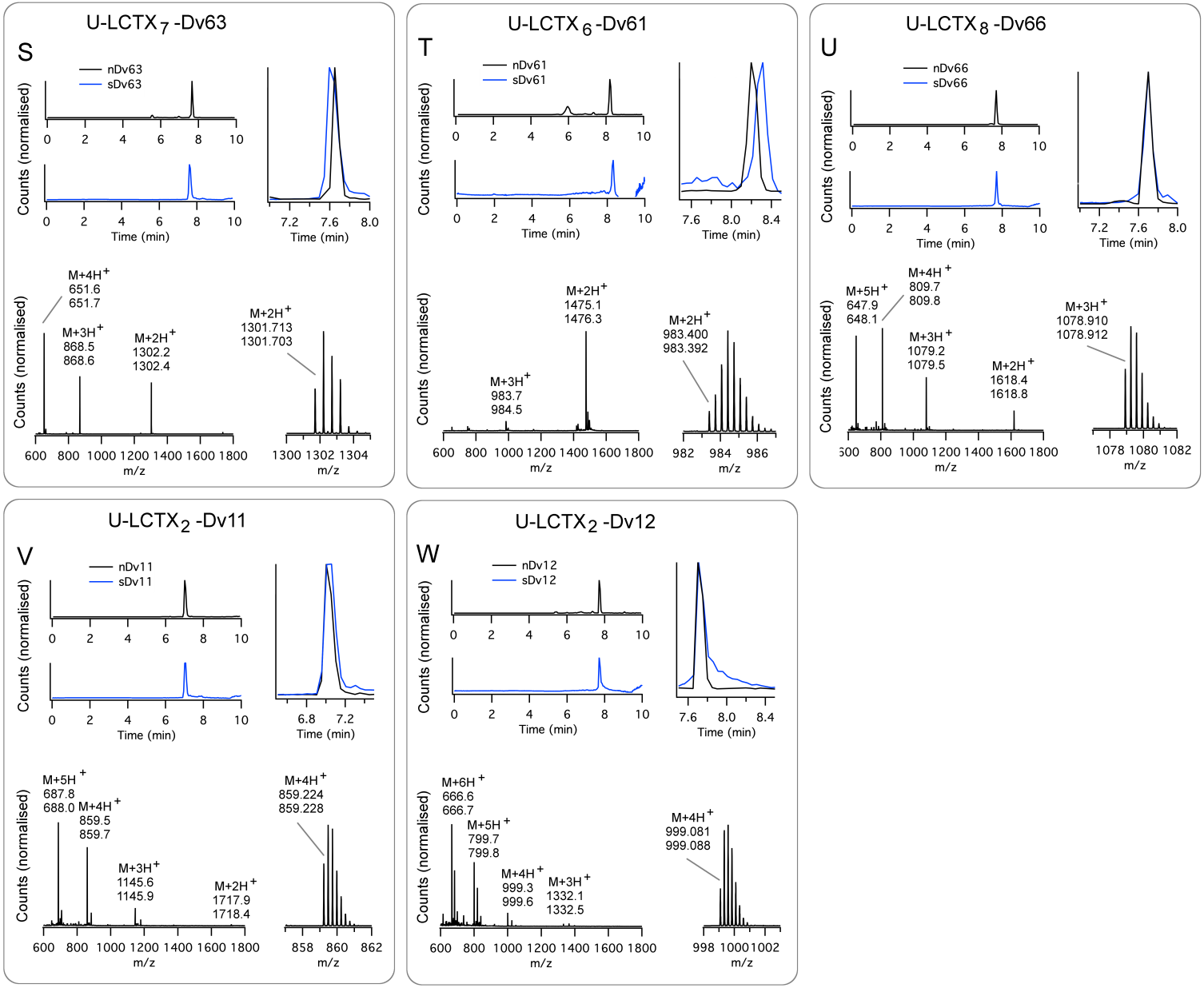
U-LCTX7-Dv63
S
nDv63
sDv63
Counts (normalised)
Time (min)
M+4H+ 651.6 651.7
M+3H+ 868.5 868.6
M+2H+ 1302.2 1302.4
M+2H+ 1301.713 1301.703
m/z
U-LCTX6-Dv61
T
nDv61
sDv61
M+2H+ 1475.1 1476.3
M+3H+ 983.7 984.5
M+2H+ 983.400 983.392
U-LCTX8-Dv66
U
nDv66
sDv66
M+5H+ 647.9 648.1
M+4H+ 809.7 809.8
M+3H+ 1079.2 1079.5
M+2H+ 1618.4 1618.8
M+3H+ 1078.910 1078.912
U-LCTX2-Dv11
V
nDv11
sDv11
M+5H+ 687.8 688.0
M+4H+ 859.5 859.7
M+3H+ 1145.6 1145.9
M+2H+ 1717.9 1718.4
M+4H+ 859.224 859.228
U-LCTX2-Dv12
W
nDv12
sDv12
M+6H+ 666.6 666.7
M+5H+ 799.7 799.8
M+4H+ 999.3 999.6
M+3H+ 1332.1 1332.5
M+4H+ 999.081 999.088

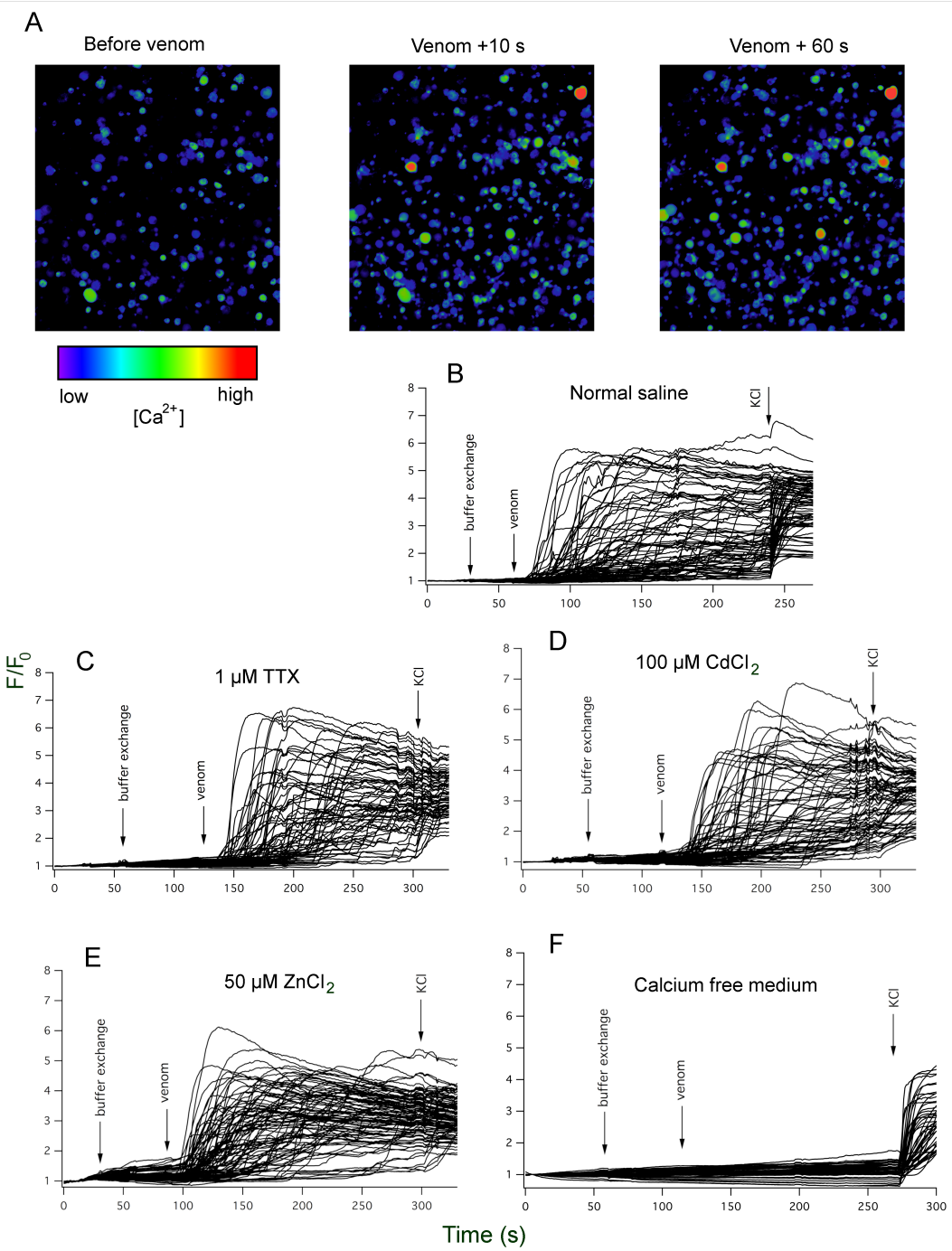

Fig. S6: Venom-induced calcium influx into DRG cells. (**A**) Photomicrographs of DRG cells before, 10 s after, and 1 min after application of 100 ng/µL venom. (**B**) Resulting calcium influx measured as an increase in fluorescence relative to initial fluorescence (F/F_0). Each trace corresponds to one cell. (**C–E**) Venom-induced calcium influx occurred in the presence of tetrodotoxin (TTX), a blocker of voltage-gated sodium (Na_V) channels, and Cd^{2+} and Zn^{2+}, blockers of voltage-gated calcium (Ca_V) channels, indicating that TTX-sensitive Na_V channels, and Ca_V channels, are not necessary for this calcium influx. (**F**) Removal of Ca^{2+} from the extracellular medium prevented calcium influx, indicating that the observed increase in intracellular calcium is due to influx across the plasma membrane rather than release from intracellular stores.

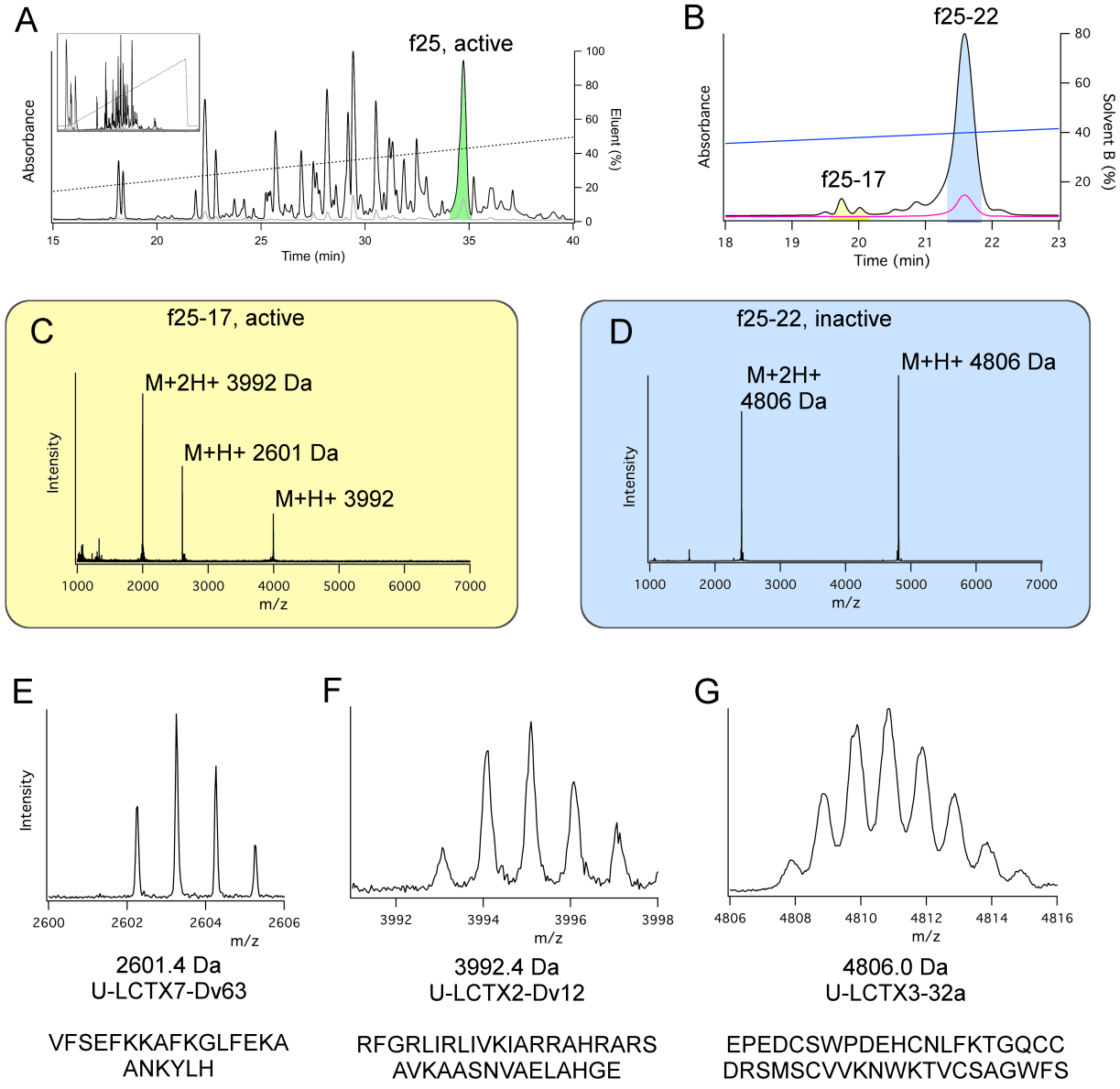

Fig. S7: Assay-guided fractionation of venom to identify algogenic (pain-inducing) molecules. (**A**) Chromatogram from C18 RP-HPLC fractionation of *D. vulnerans* venom. Testing of individual RP-HPLC fractions for their ability to activate DRG cells revealed one late-eluting fraction, fraction 25 (f25, green), with potent activity. (**B**) Further fractionation of f25 using a more gradual RP-HPLC gradient revealed the pure major component f25-22 as well as minor components in fraction f25-17. Panels C–G show MALDI-TOF mass spectra of these venom components. (**C**) f25-17 was found to be active and contained two peptides with monoisotopic masses 3992.4 Da and 2601.4 Da. (**D**) f25-22 was found to be inactive and contained one peptide with mass 4806.0 Da. (**E–G**) MALDI-TOF spectra and amino acid sequences of the peptides resolved by LC-MS/MS.

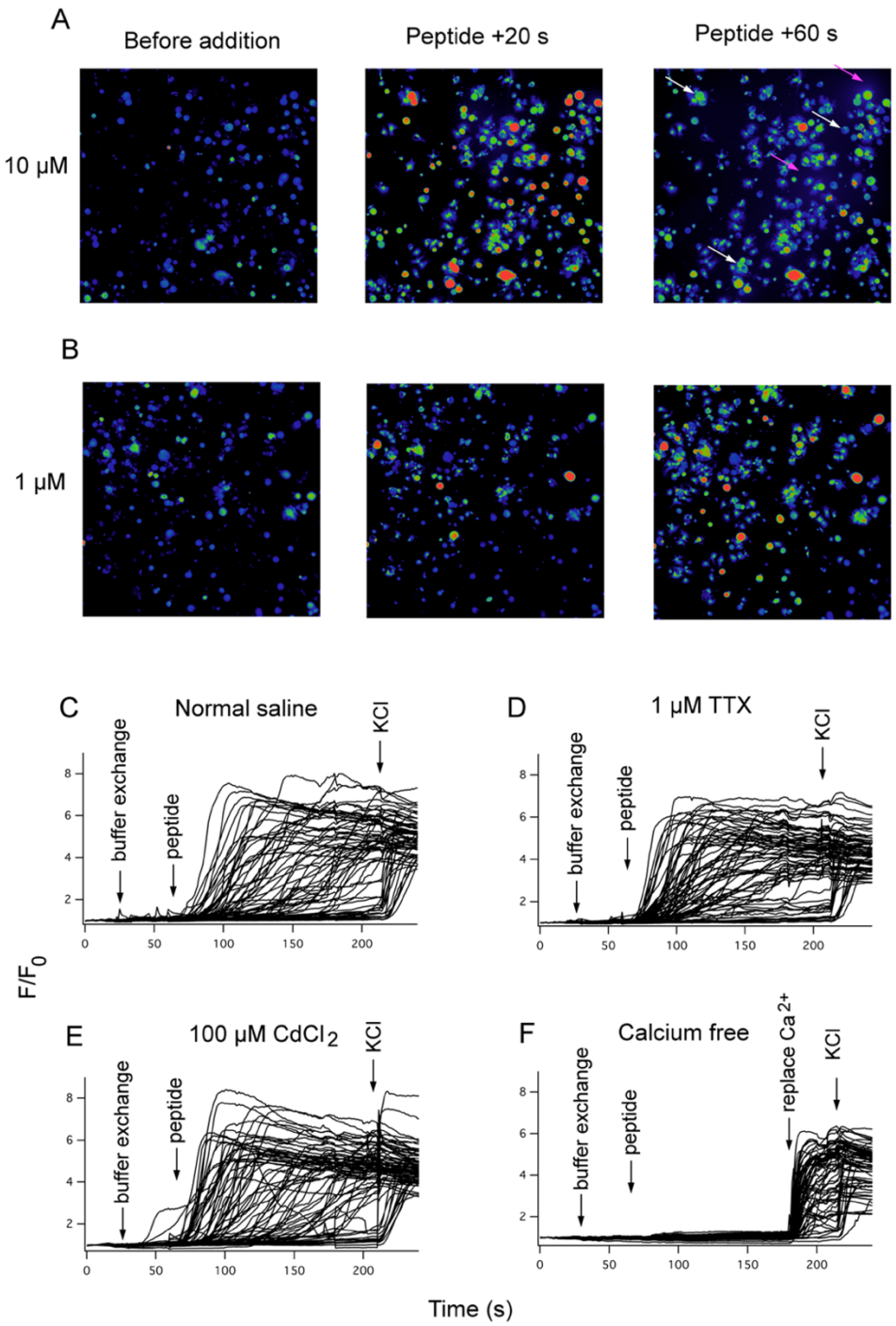

Fig. S8: Membrane disruption by synthetic Δ-LCTX$_2$-Dv12. (**A**) Photomicrographs of DRG cells showing that application of 10 µM Dv12 causes calcium influx and dye leakage. Note the loss of fluorescent signal (white arrows) and leakage of dye from cells (pink arrows) after 60 s of exposure. (**B**) Application of 1 µM Dv12 causes calcium influx without dye leakage. (**C**) Increase of fluorescence (F) compared to initial fluorescence (F_0) for a representative sample of individual cells exposed to Dv12. Blockage of Na_V channels with 1 µM TTX (**D**) or Ca_V channels with 100 µM $CdCl_2$ (**E**) did not abolish peptide-induced calcium influx. (**F**) In Ca^{2+}-free media no influx occurs, but the membrane is permeabilized, leading to rapid influx when Ca^{2+} is returned.

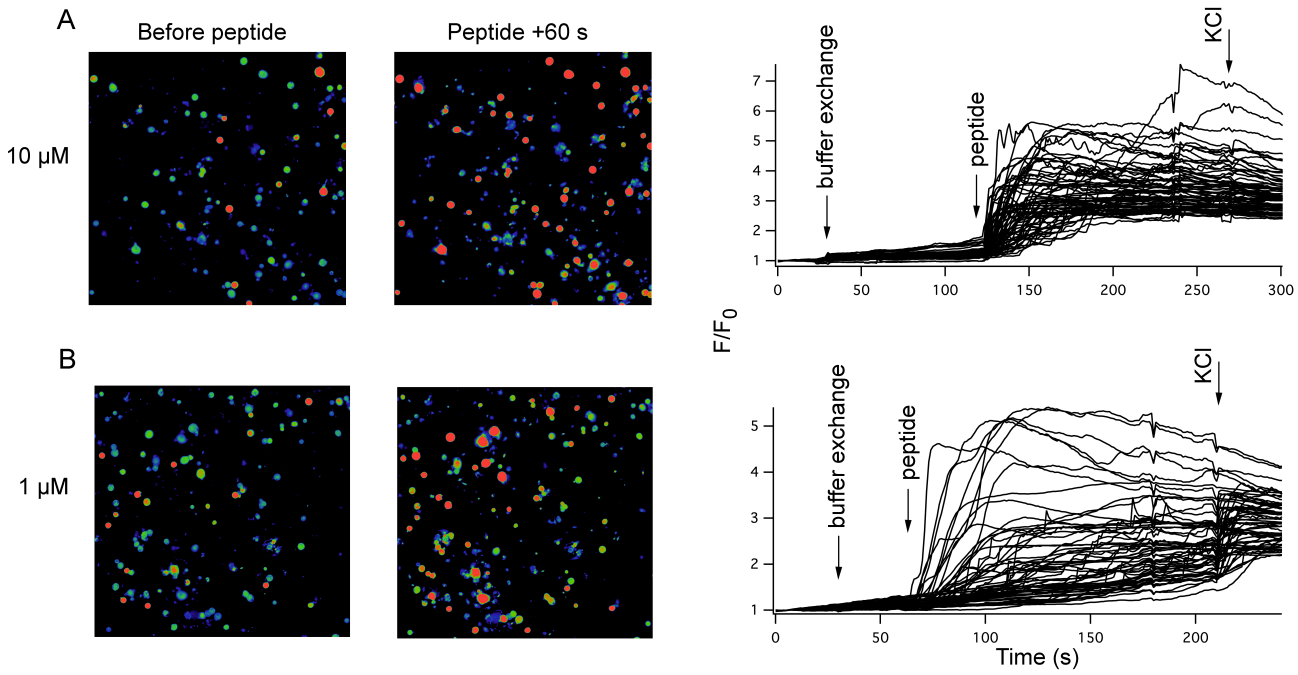

Figure S9: Calcium influx induced by exposure to Δ-LCTX$_2$-Dv11 at concentrations of (**A**) 10 µM, and (**B**) 1 µM. Format as per Fig. S7.

Table S1: Antibacterial effects of venom peptides. Table shows minimum inhibitory concentrations (MICs) in μM.

Peptide	*Staphylococcus aureus*	*Escherichia coli*	*Klebsiella pneumoniae*	*Pseudomonas aeruginosa*	*Acinetobacter baumannii*	*Candida albicans*	*Cryptococcus neoformans* var. *grubii*	Human embryonic kidney cells	Human erythrocytes
Δ-LCTX$_2$-Dv11	**16**	>32	>32	>32	**≤0.25**	>32	>32	>32	>32
Δ-LCTX$_2$-Dv12	**≤0.25**	**2**	**16**	**8**	**≤0.25**	>32	**≤0.25**	**19**[a]	**18.9**[b]
U-LCTX$_3$-Dv21	>32	>32	>32	>32	>32	>32	>32	>32	>32
U-LCTX$_3$-Dv33	>32	>32	>32	>32	>32	>32	>32	>32	>32
U-LCTX$_7$-Dv63	>32	>32	>32	>32	>32	>32	>32	>32	>32
U-LCTX$_8$-Dv66	>32	>32	>32	>32	>32	>32	>32	>32	>32
U-LCTX$_{12}$-Dv72	>32	>32	>32	>32	>32	>32	>32	>32	>32
U-LCTX$_{13}$-Dv73	>32	>32	>32	>32	>32	>32	>32	>32	>32
U-LCTX$_{14}$-Dv74	>32	>32	>32	>32	>32	>32	>32	>32	>32

[a]Concentration at which 50% cytotoxicity is observed.
[b]Concentration at which 10% hemolysis is observed.

Table S2: Nematocidal effects of venom peptides. IC_{50} values and resistance ratios for effects of caterpillar venom peptides and commercial anthelmintics on drug-susceptible (Kirby) and drug-resistant (MPL-R) isolates of *H. contortus*.

Peptide or commercial anthelmintic	Kirby		MPL-R		Resistance ratio[b]
	IC_{50} (μM)[a]	95% CI	IC_{50} (μM)[a]	95% CI	
U-LCTX$_3$-Dv33	**2.6**	2.0–3.2	**3.4**	2.2–5.1	nd
U-LCTX$_3$-Dv21	22.1	18.2–26.8	22.8	19.1–27.7	nd
Δ-LCTX$_2$-Dv12	24.5	15.5–38.1	31.4	20.2–49.2	nd
Δ-LCTX$_2$-Dv11	30.5	24—38.3	32.0	26.1—38.9	nd
U-LCTX$_7$-Dv63	41.3	29.3–71.1	48.5	35.5–140.1	nd
U-LCTX$_{13}$-Dv73	94.5	-	>100	-	nd
U-LCTX$_6$-Dv61	>100	-	>100	-	nd
U-LCTX$_{14}$-Dv74	>100	-	>100	-	nd
U-LCTX$_{12}$-Dv72	>100	-	>100	-	nd
U-LCTX$_8$-Dv66	>100	-	>100	-	nd
Levamisole	0.42	0.36–0.49	0.79	0.61–1.03	1.9
Monepantel[c]	6.64	4.85–9.10	70.84	24.56–204.3	10.7
			10950	8185–14640	1650
Ivermectin	0.26	0.24–0.30	0.63	0.58–0.71	2.4
Thiabendazole	0.065	0.060–0.070	1.09	0.94–1.75	17

[a]IC_{50} units are μM for peptides, levamisole and thiabendazole, and nM for ivermectin and monepantel.

[b]Resistance ratio = IC_{50} MPL-R isolate / IC_{50} Kirby isolate; 'nd' indicates that IC_{50} values were not significantly different between the Kirby and MPL-R isolates, based on overlap of 95 % CIs.

[c]From A. Raza et al. (11). IC_{50} values for monepantel with the MPL-R isolate represent subpopulations showing low- and high-level resistance to this anthelmintic.

Movie S1 (separate file): Defensive spine eversion by *D. vulnerans* and *D. quadriguttata*.

Dataset S1 (separate file): Excel spreadsheet with detailed sequences and annotation of venom proteome of *D. vulnerans*.

SI References

1. B. J. Haas *et al.*, *De novo* transcript sequence reconstruction from RNA-seq using the Trinity platform for reference generation and analysis. *Nat. Protocols* **8**, 1494–1512 (2013).
2. T. N. Petersen, S. Brunak, G. von Heijne, H. Nielsen, SignalP 4.0: discriminating signal peptides from transmembrane regions. *Nat. Methods* **8**, 785–786 (2011).
3. R. D. Finn, J. Clements, S. R. Eddy, HMMER web server: interactive sequence similarity searching. *Nucleic Acids Res.* **39**, W29–37 (2011).
4. N. J. Saez, B. Cristofori-Armstrong, R. Anangi, G. F. King, "A strategy for production of correctly folded disulfide-rich peptides in the periplasm of *E. coli*" in Heterologous Gene Expression in *E. coli*: Methods and Protocols, N. A. Burgess-Brown, Ed. (Springer, New York, USA, 2017), 10.1007/978-1-4939-6887-9_10, pp. 155–180.
5. F. W. Studier, Protein production by auto-induction in high density shaking cultures. *Protein Expr Purif* **41**, 207–234 (2005).
6. A. Wahedi, G. Gäde, J.-P. Paluzzi, Insight into mosquito GnRH-related neuropeptide receptor specificity revealed through analysis of naturally occurring and synthetic analogs of this neuropeptide family. *Frontiers in endocrinology* **10**, 742–742 (2019).
7. A. Oryan, A. Wahedi, J.-P. V. Paluzzi, Functional characterization and quantitative expression analysis of two GnRH-related peptide receptors in the mosquito, *Aedes aegypti*. *Biochem. Biophys. Res. Commun.* **497**, 550–557 (2018).
8. J.-P. V. Paluzzi *et al.*, Investigation of the potential involvement of eicosanoid metabolites in anti-diuretic hormone signaling in *Rhodnius prolixus*. *Peptides* **34**, 127–134 (2012).
9. A. Wahedi, J.-P. Paluzzi, Molecular identification, transcript expression, and functional deorphanization of the adipokinetic hormone/corazonin-related peptide receptor in the disease vector, *Aedes aegypti*. *Sci. Rep.* **8**, 2146–2146 (2018).
10. A. C. Kotze *et al.*, Exploring the anthelmintic properties of Australian native shrubs with respect to their potential role in livestock grazing systems. *Parasitology* **136**, 1065–1080 (2009).
11. A. Raza, J. Lamb, M. Chambers, P. W. Hunt, A. C. Kotze, Larval development assays reveal the presence of sub-populations showing high- and low-level resistance in a monepantel (Zolvix®)-resistant isolate of *Haemonchus contortus*. *Vet. Parasitol.* **220**, 77–82 (2016).
12. A. Y. Kawahara *et al.*, Phylogenomics reveals the evolutionary timing and pattern of butterflies and moths. *Proc. Natl. Acad. Sci. USA* **116**, 22657–22663 (2019).
13. W. Huang, K. Dolmer, P. G. W. Gettins, NMR solution structure of complement-like repeat CR8 from the low density lipoprotein receptor-related protein. *J. Biol. Chem.* **274**, 14130–14136 (1999).
14. S. Li, Q.-R. Zhang, W.-H. Xu, D. A. Schooley, Juvenile hormone diol kinase, a calcium-binding protein with kinase activity, from the silkworm, *Bombyx mori*. *Insect Biochem. Mol. Biol.* **35**, 1235–1248 (2005).
15. T. J. Nelson *et al.*, Calexcitin: A signaling protein that binds calcium and GTP, inhibits potassium channels, and enhances membrane excitability. *Proc. Natl. Acad. Sci. USA* **93**, 13808–13813 (1996).